ChemComm

An extended-gate-type organic transistor for monitoring the Menschutkin reaction of tetrazole at a solid-liquid interface

Journal:	*ChemComm*
Manuscript ID	CC-COM-07-2024-003266.R2
Article Type:	Communication

ChemComm

COMMUNICATION

An extended-gate-type organic transistor for monitoring the Menschutkin reaction of tetrazole at a solid-liquid interface

Received 00th January 20xx,
Accepted 00th January 20xx

DOI: 10.1039/x0xx00000x

Yui Sasaki, [a,b,c] Kohei Ohshiro, [b] Xiaojun Lyu, [b] Takayuki Kawashima, [b] Masao Kamiko, [b] Hikaru Tanaka, [d] Akari Yamagami, [d] Yoshinori Ueno [d] and Tsuyoshi Minami*[b]

We herein propose an approach to visualize Menschutkin reaction at an interface between a self-assembled monolayer with a nucleophilic property and water containing alkyl halides. An organic field-effect transistor functionalized with the nucleophilic monolayer has detected *in-situ* alkylation depending on differences in leaving group ability and bulkiness of electrophilic alkyls.

Self-assembled monolayers (SAMs) have unique properties derived from intermolecular interactions among building blocks.[1] SAMs are formed on solid-state substrates by various methods such as vapor deposition and wetting processes.[2] The fabrication methods involve the chemistry of SAMs, which affect growth, nucleation, and coalescence.[3] In this regard, *in-situ* chemical modification on SAM-attached substrates effectively endows functions with SAMs on demand.[4] Surace analysis to identify SAM modification is performed using X-ray photoelectron spectroscopy (XPS) and Raman spectroscopy.[4] However, facile methods for monitoring chemical reactions on SAMs have not been fully established. Therefore, we propose a sensor device to detect chemical reactions on SAMs.

An organic field-effect transistor (OFET) is a solution-processable electronic device.[5,6] The switching characteristics of OFETs are observed upon applying gate voltages. In this regard, the surface potentials of gate electrodes are manipulated by SAM modification, which affects the performance of OFETs.[7] Upon chemical reactions on SAM-attached electrodes, changes in structure of SAMs cause the difference in surface potentials. Thus, chemical reactions on SAMs modified on gate electrodes can be detected through changes in transistor characteristics (i.e., drain currents (I_{DS}s) and threshold voltages (V_{TH}s)).[7] In this study, we applied an extended-gate structure[8] for an OFET to detect structure changes of SAMs upon *in-situ* chemical reactions at a solid-liquid interface.

Herein, we employed the Menschutkin reaction to discuss the reactivity based on differences in 1) leaving group ability and 2) bulkiness of electrophilic alkyls (Fig. 1(a)).[9] The nucleophilic substitution reaction *in-situ* has been monitored using self-assembled materials in solution states,[9b, 9c] whereas the reaction has never been applied to SAMs at solid-liquid interfaces. To detect alkylation using the OFET, 1-hydroxyethyl-5-mercapto-1*H*-tetrazole (EMT) as a nucleophile was modified on the extended-gate electrode (Fig. 1(b)). Tetrazole is the representative heterocyclic structure comprising four nitrogen atoms, the nucleophilicity of which is a potent property in drug discovery.[10] π Electrons of the tetrazole ring are delocalized, whereas the substitution cause influences π systems.[11] Thus, the changes in charges around the tetrazole ring on the extended-gate electrode can be referred to as signals of alkylation. A tetrazole ring thiolated at the 5 position was

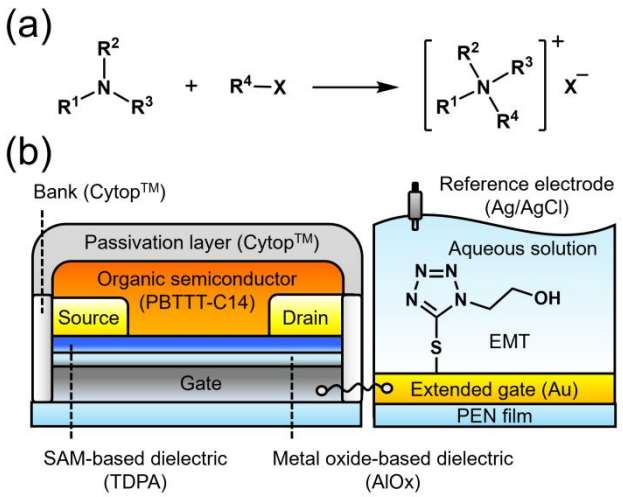

Fig. 1 (a) General scheme of the Menschutkin reaction. (b) Scheme of Schematic illustration of the extended-gate-type OFET sensor functionalized with a tetrazole derivative (i.e., 1-hydroxyethyl-5-mercapto-1*H*-tetrazole, EMT for detecting *in-situ* alkylation at the solid-liquid interface.

[a] *Research Center for Advanced Science and Technology, The University of Tokyo, 4-6-1, Komaba, Meguro-ku, Tokyo,153-8904 Japan*
[b] *Institute of Industrial Science, The University of Tokyo, 4-6-1 Komaba, Meguro-ku, Tokyo, 153-8505, Japan. E-mail: tminami@g.ecc.u-tokyo.ac.jp*
[c] *JST, PRESTO, 4-1-8 Honcho, Kawaguchi, Saitama, 332-0012, Japan*
[d] *Corporate Research Center, Toyobo Co., Ltd., 2-1-1 Katata, Otsu, Shiga, Japan*
Electronic Supplementary Information (ESI) available: [Regents and materials, apparatuses, fabrication and operation of the OFET, fabrication and characterization of the extended-gate Au electrode, time-dependency test, identification of an alkylated EMT derivative, selectivity test, and semi-quantitative assay]. See DOI: 10.1039/x0xx00000x

selected as a building block, considering the following aspects. A hydroxyethyl group introduced into the tetrazole ring at the 1 position can provide intermolecular interactions among building blocks immobilized as a SAM, which contributes uniform SAM.[12] Meanwhile, a substitution reaction at the 4 position of the tetrazole ring occurs in a 1,5-substituted derivative.[13] Therefore, the alkylation near the electrode surface can be detected sensitively using the OFET. In this study, the transistor characteristics of the EMT-attached OFET upon alkylation were analyzed using principal component analysis (PCA) to visualize the reactivity of the EMT-based SAM using alkyl halides.

The OFET was fabricated step-by-step (See the Electronic Supplementary Information, ESI†). A double dielectric layer made of aluminum oxide (AlOx) and tetradecylphosphonic acid (TDPA) was employed to achieve device operation at low voltages (<|3| V).[14] A π-conjugate polymer, poly{2,5-bis(3-tetradecylthiophen-2-yl)thieno[3,2-*b*]thiophene} (PBTTT-C14)[15] was drop cast onto a channel region. A hydrophobic material (i.e., CYTOP™) as a passivation layer was entirely covered on the surface of the OFET device for stable operation under ambient conditions (Figs. S1 and S2, ESI†).

The extended-gate Au electrode was fabricated on a polyethylene naphthalate (PEN) film through thermal deposition using a shadow mask. The Au electrode surface was functionalized with EMT under ambient conditions (See the ESI†). The molecular density of EMT was estimated by linear sweep voltammetry, resulting in (1.76±0.44)×10^{-10} mol/cm^2 (n = 3) (Fig. S3, ESI†). Photoelectron yield spectroscopy (PYS) in air was performed to estimate the work functions of the Au electrode before (4.89±0.04 eV) and after modification of EMT (4.76±0.02 eV) (Fig. S4, ESI†). The shift in the work function to a shallow direction indicates the accumulation of electron-donating groups.[8b] In addition, an increase in surface hydrophilicity of the electrode surface functionalized with EMT was observed in a wettability test (Fig. S5, ESI†). Moreover, S 2*p* and N 1*s* core-level peaks originating from EMT were identified by XPS measurements (Fig. S6, ESI†). Overall, the modification of EMT was supported by various surface analyses.

The OFET device and EMT-attached extended-gate electrode were connected using a conductive cable to detect *in-situ* alkylation at the solid-liquid interface. The alkylation of EMT-based SAM was performed in an aqueous media containing 4-(2-hydroxyethyl)-1-piperazineethanesulfonic acid, HEPES) (100 mM) and NaCl (100 mM) at pH 7.4. The extended-gate-type OFET showed time-course negative shifts in transfer curves upon adding an alkyl halide (i.e., iodomethane, CH_3I) (100 μM) (Fig. S7, ESI†). A 90 % response was observed at 60 min in the time-dependency test. Next, the concentration-dependent test was performed using CH_3I. The transistor characteristics at each CH_3I concentration were recorded after incubation for 60 min. Shifts in V_{TH}s corresponded to the adding CH_3I concentration (Fig. 2). A limit of detection value for CH_3I was determined to be 57 ppb based on the 3σ method.[16] Alkyl halides are widely used reagents for organic synthesis owing to their high reactivity. Meanwhile, the inherent reactivity potentially causes toxicity and mutagenicity in human bodies

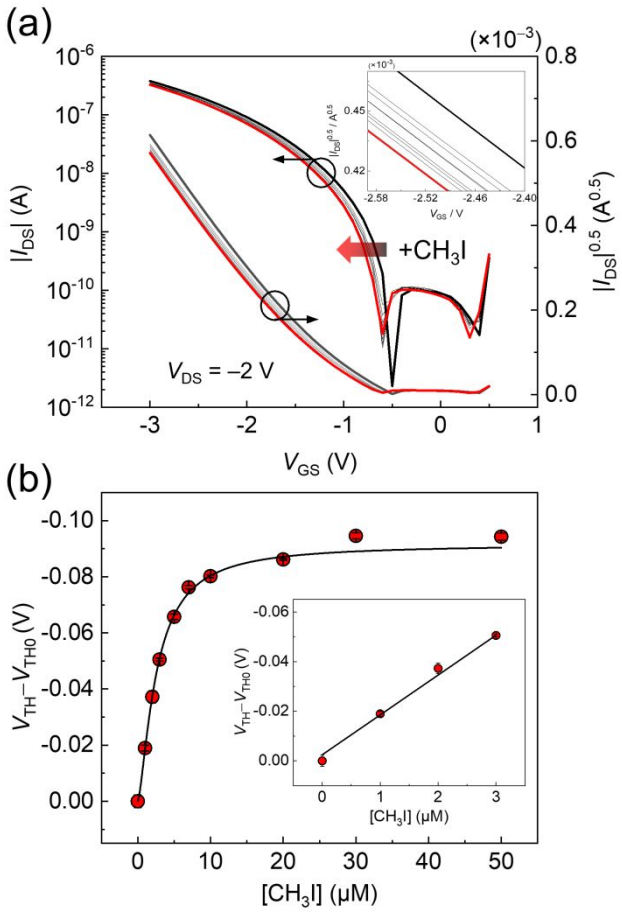

Fig. 2 (a) Transfer characteristics of the OFET functionalized with EMT upon the addition of CH_3I (0–50 μM) in 100 mM HEPES buffer with 100 mM NaCl at pH 7.4. The inset shows the enlarged figure representing changes in transfer curves. (b) The titration isotherm obtained by collecting V_{TH} at each concentration of CH_3I. The terms V_{TH0} and V_{TH} respectively indicate threshold voltages before and after adding CH_3I. Three repetitive evaluations were carried out for each concentration. The inset shows the linear relationship between changes in V_{TH} and CH_3I concentrations.

involving significant diseases.[17] Considering the demand for alkyl halide detection in an aqueous environment, the detectability of the EMT-attached OFET for alkyl halides is attractive.

Subsequently, surface analysis was performed to investigate the alkylation of the EMT-based SAM. The Au electrode functionalized with EMT was immersed in an aqueous solution containing CH_3I (100 μM) for 60 min under ambient conditions. The treated electrode was gently washed with Mili-Q water, followed by drying with a N_2 gas. Figure 3(a) represents PYS measurements of the EMT-attached Au electrode before (light pink triangle) and after the CH_3I treatment (deep pink triangle). The deeper shift of the work function implied the accumulation of positively charged species on the Au electrode.[8b] In addition, XPS measurements of the EMT-attached Au electrode treated with CH_3I supported typical peaks originating from I 3$d_{3/2}$ and I 3$d_{5/2}$ (Fig. 3(b)). Indeed, ^{1}H NMR analysis result of a mixture of 1-hydroxyethyl-5-methylthio-1*H*-tetrazole and CH_3I in a solution state shows a new peak at 4.70 ppm corresponding to

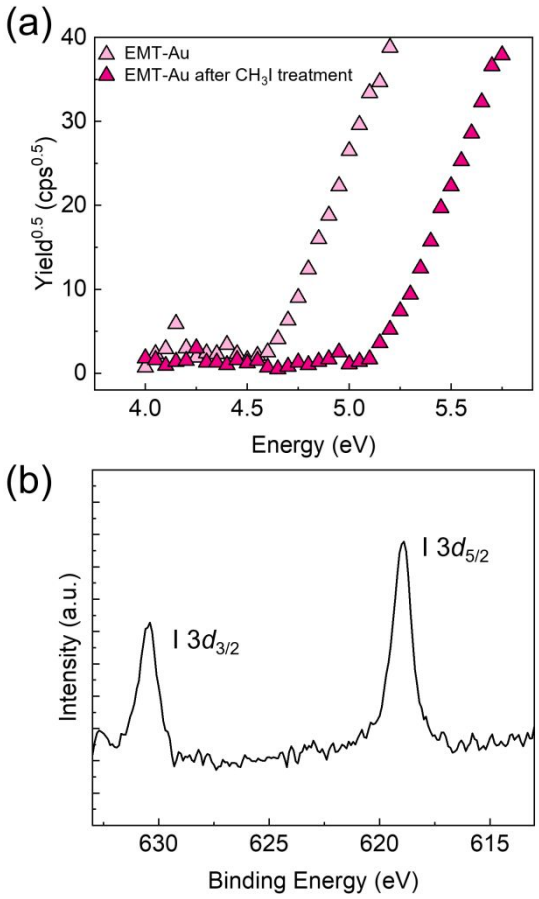

Fig. 3 (a) PYS measurements of the extended-gate Au electrode functionalized with EMT before (light pink triangle, 4.76±0.02 eV) and after the CH_3I treatment (deep pink triangle, 5.20±0.04 eV). (b) XPS core-level spectrum of I 3*d* peaks of iodine originating from EMT on the Au electrode.

methyl protons at the 4 position of the tetrazole ring (Fig. S8, ESI†).[13] Furthermore, the product after alkylation was also identified using electrospray ionization-mass spectrometry (Fig. S9, ESI†). According to evaluation in both solution and solid states, the observed changes in the transistor characteristics can be explained by the formation of tetrazolium induced by methylation.

As the next attempt, the reactivity of the EMT-attached OFET was assessed using six electrophiles (i.e., CH_3I, iodoethane (CH_3CH_2I), 2-iodopropane ($(CH_3)_2CH$-I), 2-Iodo-2-methylpropane ($(CH_3)_3C$-I), bromoethane (CH_3CH_2Br), and methyl trifluoromethanesulfonate ($CF_3SO_3CH_3$)). Figure 4 shows changes in the V_{TH} of the OFET upon adding electrophiles (5 μM). The order of V_{TH} changes implied influences of leaving group ability ($CF_3SO_3^- > I^- > Br^-$). In addition, the order depended on the bulkiness of electrophilic alkyls ($CH_3I > CH_3CH_2I > (CH_3)_2CH$-I $> (CH_3)_3C$-I).

We performed PCA to visualize the reactivity of the EMT-SAM in the Menschutkin reaction. A multidimensional dataset constructed by transistor characteristics was applied to PCA (See the ESI†). PCA can reduce the dimensionality of the dataset as two-dimensional outputs while maintaining the patterns and trends of the initial dataset.[18] PCA can determine the

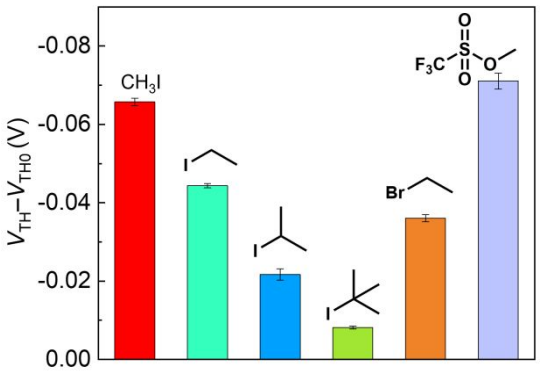

Fig. 4 Selectivity test result using six electrophiles (5 μM). The terms V_{TH0} and V_{TH} respectively indicate threshold voltages before and after adding electrophiles. Three repetitive evaluations were carried out for each measurement.

correlations between the transistor responses and analyte structures.[19] Figure 5 shows the distribution of six clusters of electrophiles at 5 μM. The position of all clusters in the PCA can be classified as dash lines according to differences in the bulkiness of electrophilic alkyls. We further demonstrated a semi-quantitative assay of six electrophiles at different concentrations using the EMT-OFET. Figure S15, ESI† represents the concentration-dependent cluster distribution by PCA.

In summary, we designed an OFET-based detection system *in-situ* for the Menschutkin reaction at a solid-liquid interface. Although *in-situ* chemical modification on SAM-attached substrates effectively endows functions with SAMs, the reactivity has not been fully discussed. Motivated by this, we aimed to discuss the reactivity of the SAM and alkyl halids based on 1) leaving group ability and 2) bulkiness of electrophilic alkyls. In this study, a hydroxyethyl group-attached tetrazole derivative, EMT was used to monitor alkylation using transistor characteristics based on conversion into a tetrazolium salt. The EMT-attached OFET showed negative shifts in the transfer curves upon adding alkyl halides, which were derived from alkylated products with positive charges. Indeed, the alkylation of the EMT-based SAM on the extended-gate electrode was supported by surface analysis using well-established

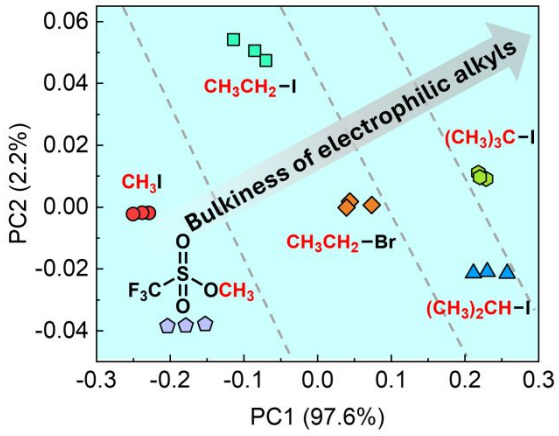

Fig. 5 PCA plot for the response patterns of six electrophiles at 5 μM. Three repetitions were carried out for each measurement.

instrumental methods. In this regard, the transistor characteristics showed unique response orders corresponding to leaving group abilities and the bulkiness of electrophilic alkyls. The responses were applied to pattern recognition for visualizing the reactivity of EMT-attached SAM and six electrophiles. All clusters in the PCA plot were distributed depending on the bulkiness of electrophilic alkyls. Overall, the EMT-attached OFET achieved not only detecting *in-situ* alkylation but also visualization of its reactivity using a data processing method. We believe the proposed method can be used for facile monitoring chemical reactions on SAMs at solid-liquid interfaces.

Y. Sasaki gratefully acknowledges the financial support from the Japan Society for the Promotion of Science (JSPS) KAKENHI (Grant No. JP24K17667) and JST PRESTO (Grant No. JPMJPR23H2). T. Minami thanks JSPS KAKENHI (Grant No. JP23H03864 and JP24K01315) and JST CREST (Grant No. JPMJCR2011). K. Ohshiro and X. Lyu thanks the JSPS Research Fellow for Young Scientists (DC1) (Grant Nos. JP23KJ0785 and JP22J23435).

Conflicts of interest

There are no conflicts of interest to declare.

Data availability

The data supporting this article have been included as part of the ESI.

References

1. (a) K. L. Prime and G. M. Whitesides, *Science*, 1991, **252**, 1164-1167; (b) E. Delamarche, B. Michel, H. A. Biebuyck and C. Gerber, *Adv. Mater.*, 1996, **8**, 713–776; (c) K. S. Mali, N. Pearce, S. De Feyter and N. R. Champness, *Chem. Soc. Rev.*, 2017, **46**, 2520–2542.
2. A. Ulman, *Chem. Rev.*, 1996, **96**, 1533–1554.
3. J. T. Woodward, I. Doudevski, H. D. Sikes and D. K. Schwartz, *J. Phys. Chem. B*, 1997, **101**, 7535–7541.
4. L. Wang, U. S. Schubert and S. Hoeppener, *Chem. Soc. Rev.*, 2021, **50**, 6507–6540.
5. G. Horowitz, *Adv. Mater.,* 1998, **10**, 365-377.
6. T. Minamiki, T. Minami, Y.-P. Chen, T. Mano, Y. Takeda, K. Fukuda and S. Tokito, *Commun. Mater.*, 2021, **2**, 8.
7. (a) K. Ohshiro, Y. Sasaki, Q. Zhou, P. Didier, T. Nezaki, T. Yasuike, M. Kamiko and T. Minami, *Chem. Commun.*, 2022, **58**, 5721–5724; (b) Y. Sasaki, Y. Zhang, K. Ohshiro, K. Tsuchiya, X. Lyu, M. Kamiko, Y. Ueno, H. Tanaka and T. Minami, *Faraday Discuss.*, 2024, **250**, 60–73.
8. (a) R. Kubota, Y. Sasaki, T. Minamiki and T. Minami, *ACS Sens.*, 2019, **4**, 2571–2587; (b) R. Mitobe, Y. Sasaki, W. Tang, Q. Zhou, X. Lyu, K. Ohshiro, M. Kamiko and T. Minami, *ACS Appl. Mater. Interfaces*, 2022, **14**, 22903–22911.
9. (a) S.-D. Yoh, D.-Y. Cheong and O.-S. Lee, J. Phys. Org. Chem., 2003, **16**, 63–68; (b) B. W. Purse, A. Gissot and J. Rebek, *J. Am. Chem. Soc.*, 2005, **127**, 11222–11223; (c) K. J. Stanger, J.-J. Lee and B. D. Smith, *J. Org. Chem.*, 2007, **72**, 9663–9668.
10. N. Dhiman, K. Kaur, V. Jaitak, *Bioorg. Med. Chem.*, 2020, **28**, 115599.
11. N. Sadlej-Sosnowska, *J. Org. Chem.*, 2001, **66**, 8737–8743.
12. (a) R. S. Clegg and J. E. Hutchison, *Langmuir*, 1996, **12**, 5239–5243; (b) P. A. Lewis, R. K. Smith, K. F. Kelly, L. A. Bumm, S. M. Reed, R. S. Clegg, J. D. Gunderson, J. E. Hutchison and P. S. Weiss, *J. Phys. Chem. B*, 2001, **105**, 10630–10636.
13. I. Yu. Shirobokov, M. V. Chekushina, V. A. Ostrovskii, G. I. Koldobskii and G. B. Erusalimskii, *Tetrazoles. 24. Preparation of 1,4-dimethyl- and 2,4-dimethyl-5-aryltetrazolium salts* in Chemistry of Heterocyclic Compounds, Springer, Berlin, 1988, **24**, 413–417.
14. H. Klauk, U. Zschieschang, J. Pflaum and M. Halik, *Nature*, 2007, **445**, 745–748.
15. I. McCulloch, M. Heeney, C. Bailey, K. Genevicius, I. MacDonald, M. Shkunov, D. Sparrowe, S. Tierney, R. Wagner, W. Zhang, M. L. Chabinyc, R. J. Kline, M. D. McGehee and M. F. Toney, *Nat. Mater.*, 2006, **5**, 328–333.
16. J. N. Miller and J. C. Miller, Statistics and Chemometrics for Analytical Chemistry, Pearson/Prentice Hall, Upper Saddle River, NJ, 2005.
17. (a) Y. Gannot, C. Hertzog-Ronen, N. Tessler and Y. Eichen, *Adv. Funct. Mater.*, 2010, **20**, 105–110; (b) W. Chen, S. A. Elfeky, Y. Nonne, L. Male, K. Ahmed, C. Amiable, P. Axe, S. Yamada, T. D. James, S. D. Bull and J. S. Fossey, *Chem. Commun.*, 2011, **47**, 253–255; (c) M.-G. Kang, H. Lee, B. H. Kim, Y. Dunbayev, J. K. Seo, C. Lee and H.-W. Rhee, *Chem. Commun.*, 2017, **53**, 9226–9229.
18. P. Anzenbacher, Jr., P. Lubal, P. Buček, M. A. Palacios and M. E. Kozelkova, *Chem. Soc. Rev.*, 2010, **39**, 3954–3979.
19. Y. Liu, T. Minami, R. Nishiyabu, Z. Wang and P. Anzenbacher, Jr., *J. Am. Chem. Soc.*, 2013, **135**, 7705–7712.

Data availability statements

The data supporting this article have been included as part of the Supplementary Information.